Determination of the oxidation state of antimony, iron and vanadium in mixed vanadium and iron antimonate oxide catalysts

D.L. Nguyen*, Y.B. Taarit, and J.-M.M. Millet

Institut de Recherches sur la Catalyse, CNRS, associé a l'Université Claude-Bernard, Lyon I, 2 Av. Albert Einstein, 69626 Villeurbanne, France

Received 21 February 2003; accepted 25 June 2003

Vanadium and mixed vanadium and iron antimonates with rutile-type structures have been studied by XANES at Sb L_1 edge, ^{57}Fe Mössbauer spectroscopy and ESR spectroscopy at 77 K. The results showed that both antimony and iron remained at their highest oxidation state, i.e. Sb^{V} and Fe^{III}, whereas vanadium was present as V^{III} and V^{IV}. Two types of V^{IV} species were distinguished corresponding to well-isolated vanadyl species in distorted octahedral coordination and vanadyl species in the same coordination but close to each other and in a dipole–dipole interaction. Both V^{III} and total V^{IV} concentrations decreased when the iron content increased, whereas isolated V^{IV} concentration increased first and then decreased, with a maximum for $x = 0.2$ in $Fe_xV_{1-x}SbO_4$. The observed variations in cationic composition are discussed in relation with the catalytic properties of the compounds in the ammoxidation of propane. Isolated V^{IV}-O moieties appeared to be the most active and selective catalytic sites.

KEY WORDS: propane; ammoxidation; acrylonitrile; vanadium and iron antimonate; ESR; XANES Mössbauer.

1. Introduction

Vanadium antimonate with rutile-type structures has recently been shown to be an active and selective catalyst for the ammoxidation of propane into acrylonitrile [1–2]. The development of industrial processes on the basis of these catalysts has generated many studies on the effect of various additives to this phase. Al, Fe, Ti and group VI transition metals have been shown to enter in the active phase structure and to modify to various degree the activity and selectivity of the catalysts [3–8]. Previous studies have shown that the substitution at low level of vanadium by iron in the rutile-type antimonate structure generated very active sites for propane oxidation [7]. Fe^{III} substituting V^{IV} in the cationic deficient structure $V^{4+}_{0.64}V^{3+}_{0.28}Sb^{5+}_{0.92}\square_{0.16}O_4$ led to a structure with both cationic and anionic vacancies: $Fe^{3+}_{x}V^{4+}_{0.64-x}V^{3+}_{0.28}Sb^{5+}_{0.92}\square_{0.16}O_{4-x/2}$. It is, however, not certain that the charge balance is directly achieved by anionic vacancies or by the formation of shear defects involving ordered arrangements of face-shared octahedra that would result in the same anion deficiency. The rutile structure with close-packed anion layers would more likely accommodate such a defect than simple vacancies. At high iron loading, both the cationic and anionic vacancies' content decreased and Fe^{III} substituted V^{III} in the solid solution compounds. The study of the catalytic properties of the compounds showed that their activity increased with the vanadium substitution up to a maximum for x around 0.2 and then decreased monotonically. Concurrently, the selectivity into acrylonitrile decreased to the benefit of that of propene and then increased up to a maximum for x around 0.8. The latter increase was attributed to the isolation of the active vanadium sites by the iron cations. This conclusion was in agreement with what had been published earlier on the role of different cations on the selectivity [3,8]. The increase of activity of the catalysts at low iron concentration, which had not been observed for other cations, was attributed to the presence of both cationic and anionic vacancies. The presence of the latter vacancies was postulated to be responsible for the selectivity increase into propene at the expense of acrylonitrile [7].

Iron and vanadium mixed oxides have been studied by XANES, Mössbauer and electron spin resonance (ESR) spectroscopies; the study has been undertaken in order to better characterize the substitution mechanism of vanadium cations by iron cations and attempt to gain further structural information allowing a more precise description of the active sites of this catalytic system.

2. Experimental

The $V_{1-x}Fe_xSbO_4$ compounds have been prepared as previously described [7]. Sb_2O_3 was added to an NH_4VO_3 and $Fe(NO_3)_3 \cdot 9H_2O$ solution under stirring. The resulting mixture was heated for 18 h under reflux and stirring. The solution was evaporated and the resulting slurry dried at 353 K before calcination in air at 623 K and 973 K for 3 h respectively. The monophasic character of the rutile-type phases obtained has been demonstrated by X-ray diffraction and transmission

* To whom correspondence should be addressed.

1011-372X/03/0900–0065/0

electron microscopy with EDX analyses [7]. The raw formula of the compounds presented in table 1, have been determined by chemical analysis [7]. They have been shown to be compatible with the characterization data obtained using several techniques like infrared and Mössbauer spectroscopy or X-ray absorption [7].

Sb L_1 XANES spectra were collected at the LURE synchrotron facility (Orsay, France). The spectra were collected at 300 K. The recording and fitting methods used have been described in Millet *et al.* [9]. $SbPO_4$ and $FeSbO_4$ reference spectra were taken as model data for Sb^{III} and Sb^{V} respectively. ^{57}Fe Mössbauer spectroscopy was performed at 298 K with a time mode spectrometer and a constant acceleration drive. 2 GBq $^{57}Co/Rh$ was used as radiation source.

Electron spin resonance spectra were recorded using a Varian E9 spectrometer operating in the X-band mode. Diphenylpicrylhydrazil (DPPH) was used as a reference for g-value determinations (3314 G, $g = 2.0036$) and vanadyl sulfate for spin calibration. Samples of ca. 30 mg were placed inside a quartz probe cell and analyzed at 77 K. The EPR data were directly fed into a PC to be processed as desired.

Catalytic activity measurement conditions have been described in detail in Roussel *et al.* [7]. The ammoxidation of propane was conducted at atmospheric pressure in a dynamic differential microreactor containing 0.5–1.0 g of catalyst. Reaction conditions were as follows: total flow rate 17.2 cm^3mn^{-1}; O_2/Propane/NH_3/N_2/Ne = 1/2/2/7/0.05 (Ne was used as an internal standard). The catalysts were compared at 753 K using these conditions, with different masses to keep a comparable conversion level (18%). Acetonitrile, cyanhydric acid, propene, CO and CO_2 were the by-products formed with acrylonitrile under these reaction conditions.

3. Results

To ensure and complete the characterization of the compounds, the oxidation states of antimony, iron and vanadium have respectively been studied by XANES, Mössbauer and ESR spectroscopy. The XANES spectra at the Sb L_1 edge of the 20FeVSb and 60FeVSb compounds have been recorded at 300 K and are

Table 1
Average calculated formula of the compounds calculated using the experimental characterization data of Roussel *et al.* [7]

Compound	Calculated formula
VSb	$V^{3+}_{0.28}V^{4+}_{0.64}\square_{0.16}Sb^{5+}_{0.91}O_4$
10FeVSb	$Fe^{3+}_{0.09}V^{3+}_{0.32}V^{4+}_{0.52}\square_{0.18}Sb^{5+}_{0.92}O_{3.95}$
20FeVSb	$Fe^{3+}_{0.18}V^{3+}_{0.33}V^{4+}_{0.41}\square_{0.16}Sb^{5+}_{0.92}O_{3.88}$
30FeVSb	$Fe^{3+}_{0.28}V^{3+}_{0.33}V^{4+}_{0.32}\square_{0.14}Sb^{5+}_{0.92}O_{3.90}$
40FeVSb	$Fe^{3+}_{0.38}V^{3+}_{0.34}V^{4+}_{0.23}\square_{0.10}Sb^{5+}_{0.95}O_{3.92}$
60FeVSb	$Fe^{3+}_{0.63}V^{3+}_{0.40}Sb^{5+}_{0.97}O_4$
80FeVSb	$Fe^{3+}_{0.80}V^{3+}_{0.19}Sb^{5+}_{1.01}O_4$

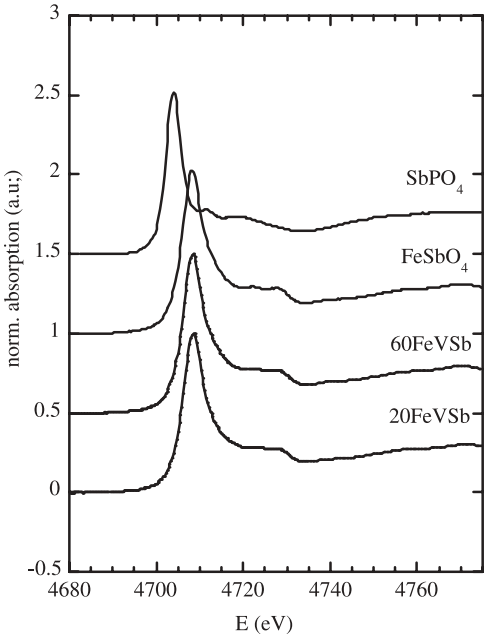

Figure 1. Normalized XANES spectra at the Sb L_1 edge of $SbPO_4$, $FeSbO_4$ and the 20FeVSb and 60FeVSb compounds.

presented in figure 1. The results showed very similar spectra for both compounds. The position of the Sb L_1 edge is sensitive to the oxidation state of antimony and the edge position of the Sb^{V} peak was systematically shifted by 4 eV to higher energies with respect to the Sb^{III} peak [9]. This appears clearly in figure 2 where the fitting of the normalized Sb L_1-edge XANES spectra of the reference compounds for Sb^{III} ($SbPO_4$) and Sb^{V} ($FeSbO_4$) were compared to that of compounds 20FeVSb and 60FeVSb. The results showed that the mixed oxide compounds contained only Sb^{V}. In both cases, the edge position of the peak was at the same

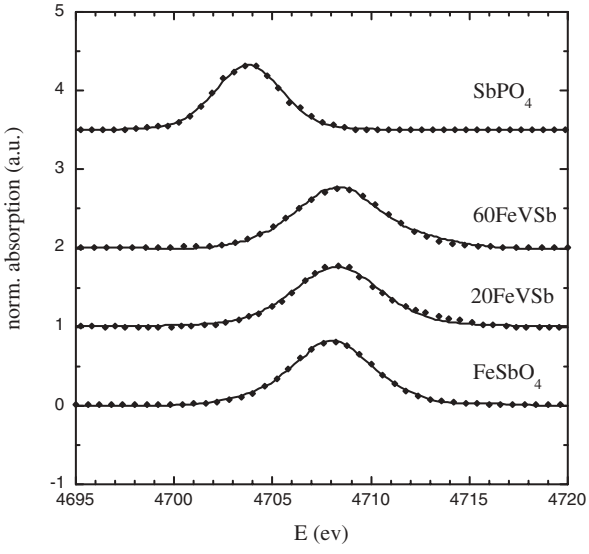

Figure 2. Fitting of the peak edge of the normalized Sb L_1-edge XANES spectra of 20FeVSb and 60FeVSb compounds with references for Sb^{III} ($SbPO_4$) and Sb^{V} ($FeSbO_4$) compounds.

energy (4708.2 eV) and corresponded to that generally observed for Sb^V [9,10].

The ^{57}Fe Mössbauer spectra of the same two compounds have been recorded at room temperature and compared to that of $FeSbO_4$ (figure 3). The three spectra have been fitted with only one doublet characterized by a $\delta = 0.34 \pm 0.01\,mm\,s^{-1}$ and $\Delta = 0.39 \pm 0.01\,mm\,s^{-1}$. These parameters were in good agreement with those published for $FeSbO_4$ [11] and were typical of paramagnetic Fe^{3+} in octahedral coordination. Analyses performed on other compounds of the solid solution showed comparable results (data not presented) [7].

The ESR spectra of $VSbO_4$ and of compounds containing iron substituting vanadium are shown in figure 4. The corresponding parameters were calculated and are presented in table 2. The spectrum of $VSbO_4$ showed two signals. The first signal was characterized by a hyperfine splitting multiplet due to ^{51}V nucleus ($I = 7/2$, 99.76%). It corresponded to well-isolated vanadyl species in distorted octahedral coordination and was well resolved (figure 5). It was superposed to a broad isotropic line, which indicated the presence of interacting vanadyl species. The overall intensity of the ESR spectrum has been measured and compared to that of a standard $VOSO_4$ solution. This calculation produced a V^{IV} content of 12.8 wt%; this value was close to that determined previously by chemical analysis and other physical techniques (14.7 wt%) [7].

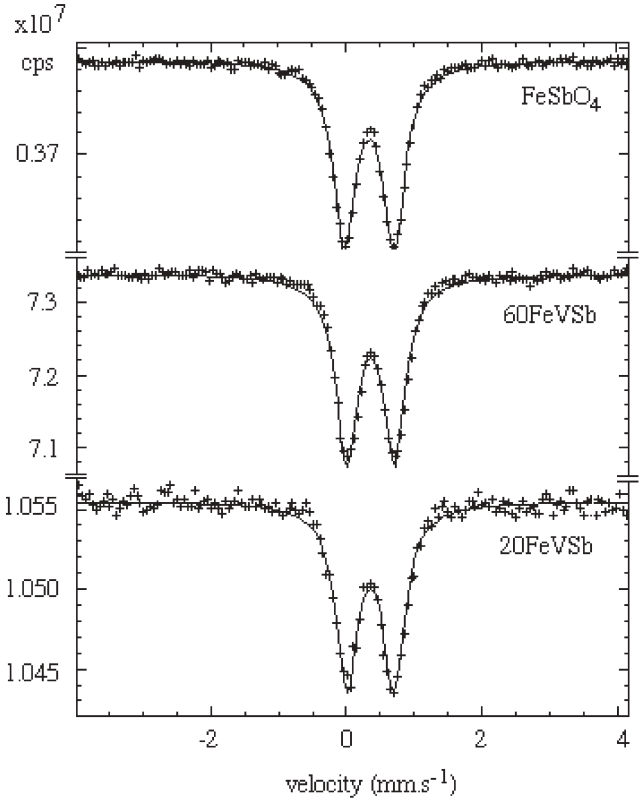

Figure 3. Mössbauer spectra of the 20FeVSb, 60FeVSb and $FeSbO_4$ compounds recorded at 298 K. Solid lines are derived from least-square fits.

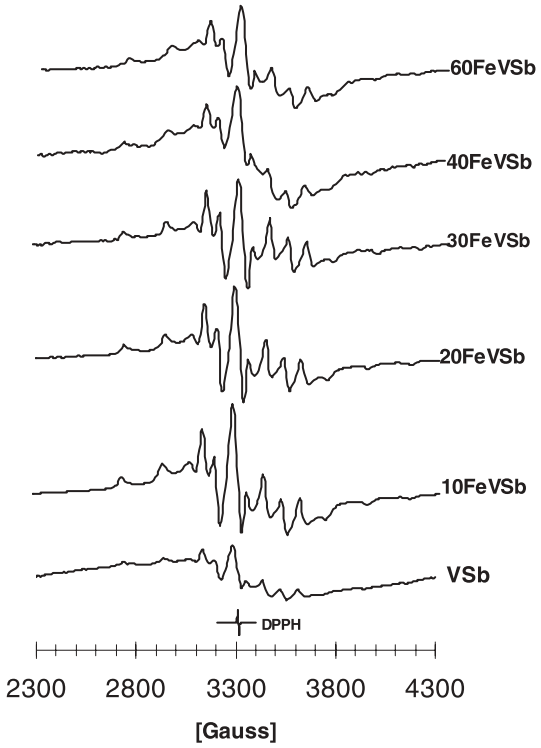

Figure 4. ESR spectra at 77 K of studied $Fe_xV_{1-x}SbO_4$ compounds.

The spectra of compounds in which iron substitutes vanadium showed the same two signals as spectrum of $VSbO_4$ (figure 4). In these compounds, $VSbO_4$ and those containing iron, the weight percent of V^{IV} (both the isolated and interacting species) have been determined from ESR analysis. This has been done by decomposing the two-signal spectra, integrating the subspectra obtained separately and calibrating them using the standard $VOSO_4$ solution; the results are presented in figure 6 (solid squares). On the basis of these values, and knowing the total vanadium content determined by chemical analyses (table 1), the ratio of V^{IV} to total vanadium (V^{IV}/V) was calculated and the influence of the composition of the catalysts on this ratio is presented in figure 6 (open squares). It can be observed that the amount of isolated V^{IV} is relatively low in $VSbO_4$. This could be explained by the high vanadium content of the compound, the elevated degree of connectivity of the rutile-type octahedral framework and by the random distribution of vanadium over the crystallographic sites that increased neighboring vanadium cations. The results also show that both the V^{IV} and the V^{IV}/V ratios decreased when the iron content of the compounds increased. The contribution of the isolated V^{IV} has been determined and, in the same manner as in the previous figure, the weight percent of isolated V^{IV} among total V^{IV} have been determined; the results are presented in figure 7 (solid squares). The ratio of isolated V^{IV} to total V^{IV} was calculated and the

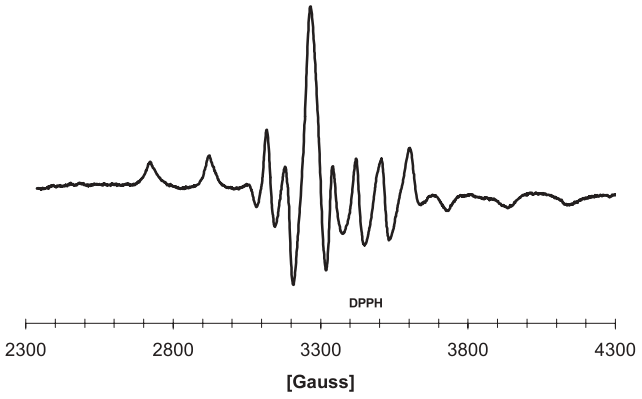

Figure 5. Enlargement of the ESR spectrum of $VSbO_4$ at 77 K after subtraction of the isotropic signal.

influence of the composition of the catalysts on this ratio is presented in the same figure (open squares). It appeared that at low iron loading, the relative amount of isolated V^{IV} increased with a maximum observed for an iron content of 0.2; beyond this content, the isolated V^{IV} decreased, reaching a minimum for an iron content of 0.4 and then increased at higher iron content. The spectrum of the richer iron compound studied (80 FeVSb) showed almost no signals.

4. Discussion

4.1. Characterization of the cationic composition of the mixed oxides

The results obtained by XANES, Mössbauer and ESR spectroscopies showed that iron and antimony have oxidation states of III and V in the mixed oxides, while vanadium has both III and IV oxidation states. They also confirmed the stoichiometries determined previously [7]. Fe^{III} preferentially substituted V^{IV} at low

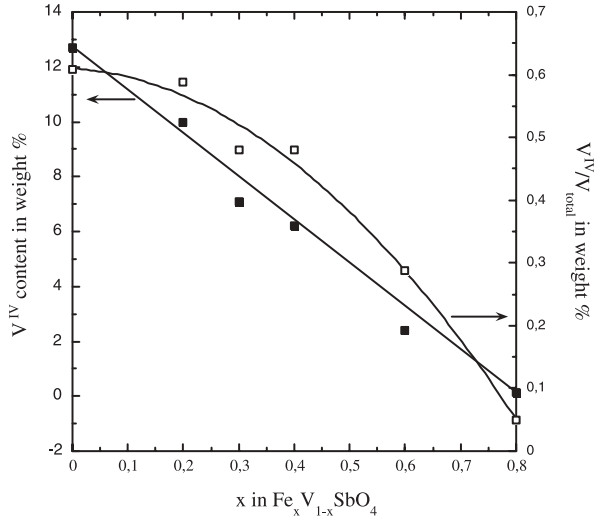

Figure 6. Variation of the amount of V^{IV} in wt% and of the relative amount of V^{IV} versus the overall amount of V in $Fe_xV_{1-x}SbO_4$ as a function of x.

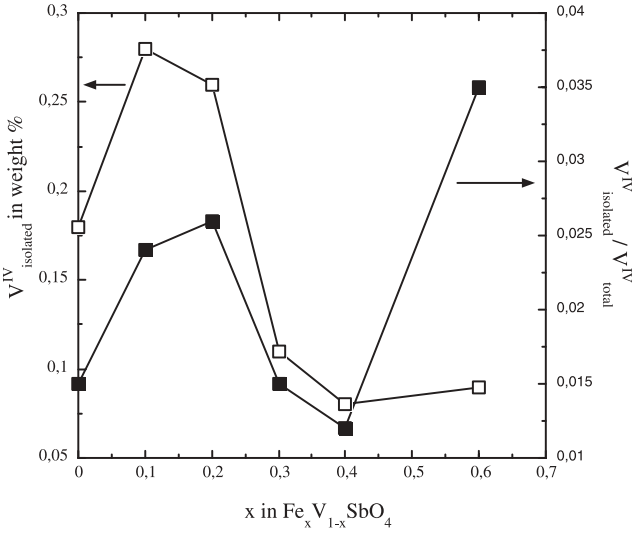

Figure 7. Variation of the total amount of isolated V^{IV} in wt% and of the relative amount of isolated V^{IV} versus total V^{IV} in $Fe_xV_{1-x}SbO_4$ as a function of x.

substitution level, and the charge balance in the compounds was achieved by point or shear defects. This was clearly shown by the decrease of the V^{IV} content observed by ESR with the substitution of vanadium by iron (figure 6). Moreover, the relative wt% of V^{IV} in the compound determined by this technique was in good agreement with that determined previously and calculated from the formula of table 1 (figure 8). ESR spectroscopy allowed to distinguish two types of V^{IV} species both in the same distorted octahedral coordination, but either isolated or neighboring and in interaction. The substitution of vanadium by iron cations brought an increase of the relative amount of isolated vanadium species with a decrease of the half width of the peaks of the corresponding signal (table 2). This was explained by the fact that Fe^{III} cations in the solid solution participated in the isolation of vanadium cations, increasing it both in terms of V–V distances and number of neighboring vanadium. When

Table 2
g and A parameters of V^{IV} signals in the mixed oxides with the half peak width of the $g_{\|}$ component of the multiplet signal (W)

x in Fe_x $V_{1-x}SbO_4$	Species	$g_{\|}$		$g_{\perp}$	$A_{\|}$ (G)	$A_{\perp}$ (G)	$W_{\|}$ (G)
0	1	1.934		1.999	202	108	37.4
	2		1.965				
0.1	1	1.933		1.999	207	105	35.4
	2		1.983				
0.2	1	1.927		1.994	205	110	34.2
	2		1.988				
0.3	1	1.934		1.995	204	105	33.9
	2		1.958				
0.4	1	1.928		1.999	199	109	37.6
	2		1.978				
0.6	1	1.927		1.993	207	105	39.2
	2		1.966				

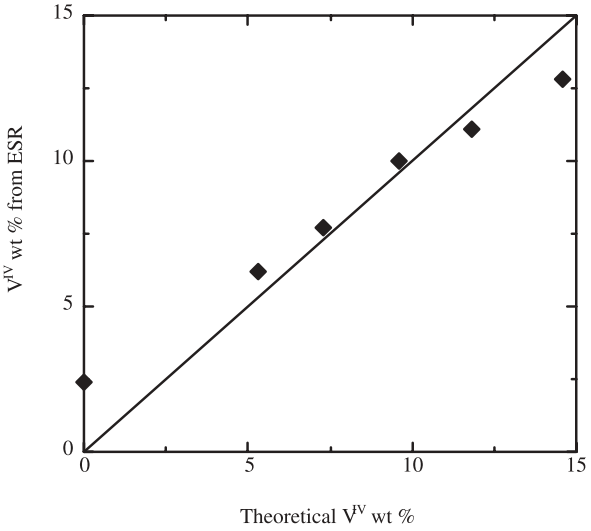

Figure 8. Variation of the relative wt% of V^{IV} in the compound determined from ESR data as a function of the theoretical one calculated from the data in table 1.

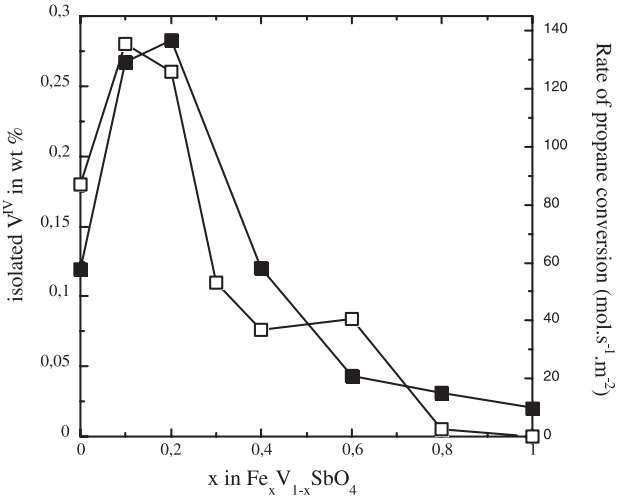

Figure 9. Comparison of the variations of the isolated V^{IV} content of (□) and of the rate of propane conversion at 753 K (■) as a function of the iron composition in $Fe_xV_{1-x}SbO_4$.

the iron content reached a certain amount (around $x = 0.2$), the defect structure was no longer stable, the defect's content started to decrease and Fe^{III} substituted V^{III}. At that point, the disappearance of cationic vacancies that were participating in the vanadium isolation led to more V–V interactions and the relative amount of isolated V^{IV} strongly decreased ($0.2 < x < 0.4$) (figure 7). At higher iron loading ($x > 0.4$) Fe^{III}–Fe^{III} spin coupling increased, creating an additional dipole–dipole interaction between unpaired vanadium and iron electrons. This gave rise to the observed increase of the half width of the peaks of the multiplet signal (table 2). In the same time the relative amount of isolated vanadium increased again as could be expected (figure 7).

4.2. Consequence for catalysis

The catalytic properties of the studied mixed oxides in the ammoxidation of propane have been previously described [7]. These published results of intrinsic rate of propane as a function of iron content have been superposed with results from this study (figure 7), expressed as a percentage of isolated V^{IV} as a function of iron content. The superposed data presented in figure 9 showed that the activity of the catalysts can be related to the isolated V^{IV} content in the compounds. Although these species have already been described as being active and selective, a clear relation such as that illustrated in figure 9 has never been reported. The relation between the cationic composition of the solid solution and the selectivity is more complex. In an attempt to illustrate this, results of the corresponding catalytic properties and ratio of isolated V^{IV} to total V^{IV} have been expressed as a function of iron content in the catalysts and superposed (figure 10). The observations are presented as a function of the range of iron substitution i.e. x in $Fe_xV_{1-x}SbO_4$.

4.2.1. $0 < x < 0.2$

At low iron loading, the number of isolated vanadium sites increased. Iron cations and also cationic vacancies participated in the site isolation. At the same time, an increase in the activity of the catalysts was observed. These species have been reported to be very selective to acrylonitrile [3]; therefore an increase of its selectivity was anticipated. However, this was not the case and instead of that an increase of the selectivity into propene was observed. In fact, a high selectivity was stated to be obtained by structural means with the isolation of V-O moieties that limited the number of available surface oxygen. However, as it has recently

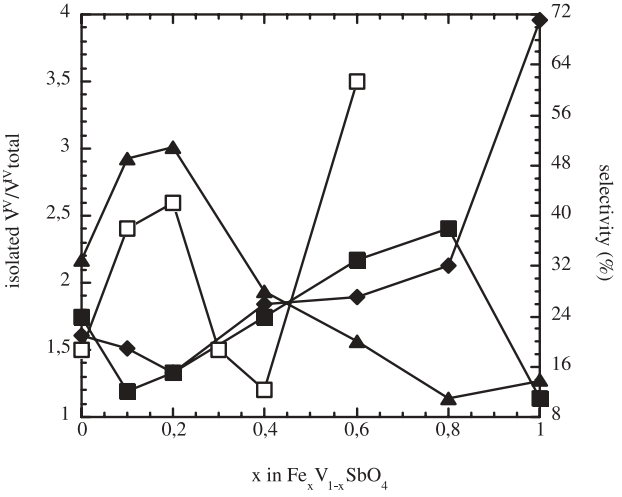

Figure 10. Comparison the relative amount of isolated V^{IV} versus total V^{IV} (□) and of the selectivity observed in propane conversion at 753 K, as a function of the iron composition in $Fe_xV_{1-x}SbO_4$; selectivity in acrylonitrile (■), propene (▲) and CO_x (◆).

been reemphasized, it is the local oxygen concentration that was the determinant parameter [12]. This is well illustrated here, where site isolation is obtained but with a concomitant lack of oxygen (anionic deficient structure) for charge balance that enabled the observation of the positive effect expected. The lower content of reactive oxygen allowed only the oxidative dehydrogenation of propane into propene, but no further dehydrogenation and possible oxidation of the alkene molecule. The reaction stopped at the oxidative dehydrogenation of propane to propene, which was confirmed to be the first intermediate in the catalytic reaction.

4.2.2. 0.2 < x < 0.4

The defective structure was stable only at low iron content; and when the iron content increased, a transformation occurred in the solid with the progressive disappearance of the vacancies and the beginning of substitution of V^{III} by Fe^{III}. Since the cationic vacancies participated in the vanadium site isolation, the number of the isolated vanadium species decreased and the activity decreased. However, since, in parallel, the oxygen repletion of the solid took place, the selectivity to acrylonitrile increased.

4.2.3. 0.4 < x < 0.8

At higher iron content, the percent of isolated V^{IV} versus total V continue to increase, but at the same time the absolute number of isolated V decreased; under these conditions, a decrease of the activity was observed. However, because the percent of isolated vanadium cations increased and because these species are selective to acrylonitrile, an increase of selectivity to acrylonitrile was observed.

4.2.4. 0.8 < x < 1.0

For these compositions, not only the total V^{IV} content but also the isolated V^{IV} content became very low. Consequently, the activity was very low and the catalytic properties were mainly those of $FeSbO_4$ with a poor activity and a dominant total oxidation of propane to CO_x.

The system studied constitutes a case study showing the importance of site isolation as has been defined by Grasselli [12]. The questions that remain are why the isolated V^{IV} species appear as the most active species, and is the concomitant presence of cationic vacancies also not a determinant parameter as proposed in Roussel *et al.* [7]. It is worthwhile to recall that cationic vacancies have already been identified at the surface of active alkane oxidation catalysts like $(VO)_2P_2O_7$ and that bulk O^- species, associated to these defects, may well allow the homolytic dissociation of the first C–H bond of an alkane molecule [7,13,14].

References

[1] A.T. Guttmann, R.K. Grasselli and J.F. Brazdil, U.S. patent 4,746,641, 4,788,317 (1988).
[2] G. Centi, R.K. Grasselli and F. Trifiro, Catal. Today 13 (1992) 661.
[3] J. Nilsson, A.R. Landa-Canovas, S. Hansen and A. Andersson, J. Catal. 160 (1996) 244.
[4] G. Centi, R.K. Grasselli, E. Patane and F. Trifiro, in: *Studies in Surface Science and Catalysis*, Vol. 55, eds. G. Centi and F. Trifiro (Elsevier, Amsterdam, 1990) p. 515.
[5] Y. Mimura, K. Ohyachi and I. Matsuura, Sci. Tech. Catal. (1998) 69.
[6] A. Wickman, L.R. Wallenberg and A. Andersson, J. Catal. 194 (2000) 153.
[7] H. Roussel, B. Mehlomakulu, F. Belhadj, E. van Steen and J.M.M. Millet, J. Catal. 205 (2002) 97.
[8] A. Andersson, J. Nilsson, C. Song and J.S. Hansen, in: *Studies in Surface Science and Catalysis*, Vol. 82, eds. V. Cortes Corberan and S. vic Bellon (Elsevier, Amsterdam, 1994) p. 293.
[9] J.M.M. Millet, E. Baca, A. Pigamo, D. Vitry, W. Ueda and J.L. Dubois, Appl. Catal. 244(2) (2003) 359.
[10] J. Rockenberger, M. Tischer, U. zum Felde, L. Tröger, M. Haase and H. Weller, J. Chem. Phys. 112(9) (2000) 4296.
[11] H. Kriegsmann, G. Öhlmann, J. Scheve and F.J. Ulrich, in *Proc. 6th Int. Congr. Catal. London*, Vol. 2, eds. G.C. Bond, P.B. Wells and F.C. Tompkins (The Chemical Society, London, 1976) p. 836.
[12] R.K. Grasselli, Top. Catal. 15(2,4) (2001) 93.
[13] J.M. Herrmann, P. Vernoux, K. Béré and M. Abon, J. Catal. 167 (1997) 106.
[14] H.H. Kung, Ind. Eng. Chem. Prod. Res. Dev. 25 (1986) 171.
[15] C. Marcu, J.M.M. Millet and J.M. Herrmann, Catal. Lett. 78 (2003) 273.